Journal of Environmental Management 282 (2021) 111950

Contents lists available at ScienceDirect

Journal of Environmental Management

journal homepage: http://www.elsevier.com/locate/jenvman

Research article

Cu(II) biosorption by living biofilms: Isothermal, chemical, physical and biological evaluation

Alireza Fathollahi [a,*], Stephen J. Coupe [a], Amjad H. El-Sheikh [b], Ernest O. Nnadi [c]

[a] Centre for Agroecology Water and Resilience (CAWR), Coventry University, Wolston Lane, Ryton on Dunsmore, CV8 3LG, UK
[b] Department of Chemistry, Faculty of Science, The Hashemite University, P.O. Box 330127, Zarqa 13133, Jordan
[c] School of Mechanical, Aerospace and Civil Engineering, The University of Manchester, M13 9PL, Manchester, UK

ARTICLE INFO

Keywords:
Toxicity
CFU
EPS
Kinetic modelling
Thermodynamics
FTIR

ABSTRACT

Dissolved copper in stormwater runoff is a significant environmental problem. Biosorption of dissolved metals using microorganisms is known as a green, low-cost and efficient method. However, the role of live biological agents in the remediation of dissolved copper in Sustainable Drainage (SuDS) has not been reported. In this study, the effect of pH, initial concentration and temperature, on bacteria in different stages of biofilm development on a geotextile, along with Cu(II) removal efficiencies, were evaluated. Maximum Cu(II) removal efficiency (92%) was observed at pH 6. By decreasing the pH from 6 to 2, a log 5 reduction in bacteria was observed and Carboxyl groups transformed from -COO^- to –COOH. The maximum biosorption capacity (119 mg g^{-1}) was detected on day 1 of biofilm development, however, maximum removal efficiency (97%) was measured on day 21 of biofilm incubation. Exteracellular Polymeric Substance (EPS) showed a better protection of CFUs in more mature biofilms (day 21) with less than 0.1 log decrease when exposed to 200 mL^{-1} Cu(II), whereas, biofilm on day 1 of incubation showed a 2 log reduction in CFUs number. Thermodynamic studies showed that the maximum Cu(II) biosorption capacity of biofilms, incubated for 7 days (117 mg g^{-1}) occurred at 35 °C. Thermodynamic and kinetic modelling of data revealed that a physical, feasible, spontaneous and exothermic process controlled the biosorption, with a diffusion process observed in external layers of the biofilm, fitting a pseudo-second order model. Equilibrium data modelling and high R^2 values of Langmuir model indicated that the biosorption took place by a monolayer on the living biofilm surface in all stages of biofilm development.

1. Introduction

Copper is one of the heavy metals with a wide range of applications including plumbing, roofing materials, cladding for buildings, cookware, electrical appliances and cables as well as agricultural inputs, being an ingredient in pesticides (Tegenaw et al., 2019). Copper compounds are also used as preservatives for wood and fabrics (Ali et al., 2017); copper can be alloyed with tin and zinc to produce bronze and brass which also have wide range of applications. Copper is an essential micronutrient, vital for human and animal health and wellbeing and as such is available in food, water, food supplements, and medications, and even contained in birth control products. Hence, the ubiquitous nature of copper makes it relatively indispensable in the modern world with increasing demand for and widening of its applications (Schipper et al., 2018). Copper is commonly found in stormwater runoff and is known to cause negative impacts in aquatic environments, particularly to fish (Hauser-Davis et al., 2014). Copper is widely available in the environment and whilst it is an essential nutrient in low concentrations when consumed, it can be toxic when ingested in higher doses (Whitfield et al., 2010). Copper toxicity is widely reported across the world and affects both humans and animals (World Health Organisation, 2004).

The EU Water Framework Directive (Directive, 2000/60/EC) and priority pollutant directive (Directive, 2013/39/EU) provided lists of pollutants in stormwater and guidelines for mitigation of diffuse pollution aimed at protecting receiving waters. Hence, due to the wide range of applications of copper in society, copper is one of the problematic pollutants in stormwater and usually occurs as particulate or in dissolved form as Cu^{2+} (Fathollahi et al., 2020a). Copper can be released into stormwater from interactions with acid rain with corroded copper products and alloys such as roofing materials, which can be categorised as total, dissolved and ionic copper concentrations. Sakson et al. (2018) observed annual mass loads of 305 g/ha/year for Cu. Stormwater runoff

* Corresponding author.
E-mail address: ad2068@coventry.ac.uk (A. Fathollahi).

https://doi.org/10.1016/j.jenvman.2021.111950
Received 9 November 2020; Received in revised form 13 December 2020; Accepted 2 January 2021
Available online 16 January 2021

from roads is recognized as a significant source of dissolved copper and reports have shown that brake pads and tyres are significant sources of copper in runoff (Mckenzie et al., 2009; Abdoli et al., 2015; Adamiec et al., 2016, Müller et al., 2020), including European Union (EU) and United Kingdom (UK) Non-exhaust emissions (NEE) reports (EU 2014; DEFRA 2019). The Department of Environmental Protection (DEP) in the State of Connecticut, USA, observed that copper levels in major natural water resources in the State exceeded the copper water quality criteria several times a year with concerns of potential copper toxicity to aquatic life (Peters 1999; Michels et al., 2002).

The risk of copper toxicity is relatively significant in domestic and recreational reuse settings, particularly amongst children (NRC 2000; ATSDR 2004; Brinks et al., 2008). Phytoaccumulation of copper from irrigation was observed to pose a risk to lettuce (Shiyab, 2018). If the option of discharging to natural water courses is adopted, then there is the risk of Cu toxicity to aquatic life and potential disruption of their ecosystem. For instance, copper is known to be toxic to arctic grayling (*Thymallus arcticus*), rainbow trout (*Oncorhynchus mykiss*) and all major populations of Coho Salmon (*Oncorhynchus kisutch)*, an aquatic organism listed as threatened or endangered under the Endangered Species Act (ESA) (NOAA 2020; USFWS 2020) at even low concentrations of 0.8–2.1 μg L^{-1}, concentrations which are widely exceeded in stormwater runoff in most countries (NOAA 2007). The occurrence of copper contamination in stormwater and its toxicity to life and environment reveals a need to understand the mechanisms of copper treatment in stormwater treatment systems such as SuDS and to appraise the efficiency of copper removal before recommending stormwater reuse options post treatment. This study aimed to examine the removal of dissolved copper, applied as Cu(II), by living microbial biofilms, grown on a relatively simple polypropylene geotextile, which is a component of most pervious pavement installations. This geotextile is known to trap and biodegrade hydrocarbons in permeable pavement systems (PPS) (Coupe et al., 2003) and has been shown to able to support a biofilm that can trap over 80% of dissolved mercury (Fathollahi et al., 2020b).

Microbial biomass is known to be an appropriate material for biosorption of copper, and a key study by Chen et al. (2005) showed that for soluble copper, the binding capacity of living cells was significantly higher (approximately double) the biosorption of non-living cells, using *Pseudomonas putida* CZ1 isolated from metal contaminated sites, in single culture. The *Pseudomonas putida* CZ1 inoculum was freely suspended in the liquid medium rather than in a biofilm and there was no attempt by Chen et al. to count the bacterial densities in the culture, or to determine the effect of different Cu concentrations on bacterial survival. The biomass of a non-living terrestrial fungus, *Aspergillus terreus,* was used in biosorption trials on copper in aqueous solution (Cerino-Córdova et al., 2012). In this study, a maximum average adsorption capacity of 268.67 (mg g^{-1}), with a removal rate of 57.45%, was recorded by the use of *A. terreus*, which was added to the Cu solution as a dried powder. Algal biosorption of Cu was measured by De Abreu (2014), with *Chlorella vulgaris* microalgae incorporating 35% of added Cu into the living cells in laboratory liquid cultures. It should be noted that 1 mg L^{-1} of Cu^{2+} was the EC_{50} for *C. vulgaris* (50% inhibition of microbial growth at 48 h), showing effects on the algal culture with relatively low concentrations.

Choudhary and Sar (2009) recorded a maximum Cu^{2+} loading of 845 nmol mg^{-1} cellular dry weight of *Pseudomonas fluorescens* grown in a liquid mineral media culture. Vullo et al., (2008) examined the effect of *Pseudomonas veronii* 2E strain, when immobilised live as a single species biofilm on teflon, silicone rubber and polyurethane growth platforms on which bacteria were surface fixed. The results showed a maximum biosorption of 40% Cu(II) at pH 5 and 6.2 with 0.5 mM Cu(II) loading.

The majority of the studies of biosorption used waste organics or dried and powdered microbial biomass, often from single species culture. The few studies that used living microbial biomass showed that functioning microbial biosorbents were more effective than deactivated controls. Studies of metal biosorption in stormwater treatment are largely absent and not recorded in PPS or with living biofilms. Therefore, this study was focused on developing a mixed culture living biofilm on a geotextile for biosorption of Cu(ll) from contaminated runoff and in order to identify biological, physical and chemical processes involved in the Cu(II) removal by the living biofilm. This study objectives were:

1. To evaluate the Cu(II) biosorption capacities and removal efficiencies of different stages of living biofilm development on a geotextile.
2. To study the Cu(II) biosorption mechanisms.
3. To carry out the toxicity of pH and different Cu(II) concentrations for all stages of biofilm growth and to evaluate the role of EPS and geotextile in protecting the bacteria.
4. Thermodynamics, kinetic and equilibrium modelling of the Cu(II) biosorption process
5. To evaluate effect of pH, temperature and initial concentrations on Cu(II) biosorption by the living biofilm.

2. Materials and methods

2.1. Bioreactor system and medium

The biofilm growth surface in this study was a 70% polypropylene and 30% polyethylene geotextile (trade name Inbitex) made by Terram, Maldon, UK. Geotextile circles of 65 surface area were prepared, washed and weighed prior to their incubation in the bioreactor to receive biofilm growth. The bioreactor used in this study was a non-transparent 15 L plastic container equipped with air pumps to keep the dissolved oxygen in the bioreactor medium in the range of 4–6 mg L^{-1} providing aerobic conditions for biofilm growth. The bioreactor medium pH was kept between 7 and 8 in a controlled room temperature of 20–25 °C. The bioreactor system was kept in the dark to prevent the growth of algae in the medium. The mixed microbial culture used in this study was naturally occurring microorganisms within the SuDS systems. The selected medium and conditions were optimized for the growth of bacteria, its attachment to the geotextile surface and development of a mature biofilm. The bioreactor medium had a composition of 9800 mL deionized water, 200 mL of mixed microbial culture isolated from a mature SuDS device at Coventry University UK, 10 g engine oil and 28 mL liquid plant food with chemical composition of 14% Nitrogen (N) and 3% phosphorus (P) for bacterial metabolism. Schematic of the bioreactor in the present study is presented in Figure Supplementary Information (SI 1).

2.2. Metal solution for biosorption

A 1000 mg L^{-1} analytical grade Cu(II) stock solution in 2% HNO_3 was used to prepare different concentrations of metal for study assays (provided by Perkin Elmer, Massachusetts, United States).

2.3. Effect of pH on biosorption and CFUs

The effect of Cu(II) solution pH on biosorption capacity and the removal efficiency of the living biofilm was tested. The metal solution pH values were adjusted by 0.5M NaOH solution and ranged between 2 and 7. A 98% pure analytical grade NaOH (provided by Sigma Aldrich, St. Louis, MO) was used to prepare the 0.5M NaOH solution.

Bacterial communities are vulnerable to experimental conditions. In order to measure the vulnerability and effect of Cu(II) on bacterial densities, expressed as Colony Forming Units per millilitre of liquid (CFUs) in different pH solutions, 0.5M NaOH was used to adjust the pH of deionized water. 10 mL of the solution was applied to 7 days incubated geotextile circles for 120 min at 25 °C. After the experiment, a 1 mL sample was taken from each treatment prior to serial dilution and nutrient agar plate counts. Agar plates were incubated for 72 h before counting the emerged colonies. Nutrient agar had the following formula:

yeast extract 2g L^{-1}, peptone 5 g L^{-1}, sodium chloride 5 g L^{-1}, agar 15 g L^{-1} with a pH of 7.4 at 25 (provided by ThermoFisher Scientific).

2.4. Effect of initial metal concentration on biosorption and CFUs

Geotextile circles were harvested from the bioreactor on day 1, 7, 14, 21 and 28 prior to the batch biosorption experiments. An adjusted amount of analytical grade Cu(II) stock solution was used to prepare 1, 5, 10, 20, 50, 100, 150 and 200 mg L^{-1} metal solutions to examine the effect of initial metal concentrations on the biosorption experiment. The pH of solutions was adjusted to 5.5 by 0.5M NaOH solution and experiments were carried out at 25 °C with 120 min contact time. The Cu(II) concentration in resulting solutions was measured using a PerkinElmer optima 5300 DV ICP-OES instrument. 1 mL of sample was taken from each treatment of geotextile circles, serially diluted and plated onto nutrient agar with the same method described in section 2.3 to evaluate the toxicity of different concentrations of Cu(II) for bacterial colonies on and detached from the geotextile circles. After harvesting the geotextile circles, different concentrations of Cu(II) were applied on top of them for 120 min prior to filtration and taking samples for ICP-OES analysis. Schematic of the batch biosorption experiments in the present study is presented in Figure SI1. Geotextile circles were dried in an oven at 60 °C for 74 h prior to weighing for biosorption capacity calculations.

After the biosorption experiments, samples were taken for ICP-OES analysis to determine the remaining (equilibrium) concentration of Cu (II) ion in solution (C_e) and then removal efficiency (R) was calculated as follows:

$$R = \frac{(C_i - C_e)}{C_i} \times 100$$

where R is removal efficiency (%), C_i is initial concentration of the solution (mg L^{-1}) and C_e is the metal concentration in the solution at equilibrium (mg L^{-1}).

Geotextile circles were then placed in the oven at 60 °C for 72 h prior to their weight measurement and biosorption capacity calculations (q_e). The Cu(II) biosorption efficiency of different stages of biofilm growth was calculated using the equation below:

$$q_e = \frac{(C_i - C_e)}{m} \times V$$

where q_e is the amount adsorbed metal ions on adsorbent surface (mg g^{-1}), m is the mass of biofilm (g) and V is the volume of the solution (L).

2.5. Effect of temperature on biosorption

Geotextile circles were harvested after 7 days of incubation and batch biosorption experiments (section 2.4) were carried out at 25 °C, 35 °C, 45 °C and 55 °C to evaluate the effect of temperature on the efficiency of the living biofilm in Cu(II) removal at pH 5.5 with 120 min contact time. Samples were taken and analysed using the ICP-OES. Thermodynamic parameters were calculated to understand the biosorption process characteristics, including feasibility and spontaneity.

2.6. Effect of contact time on biosorption

In order to evaluate the effect of contact time on the biosorption process, geotextile circles incubated for 7 days, were harvested prior to being exposed to 1, 5, 10, 20, 50, 100, 150 and 200 mg L^{-1} Cu(II) concentrations at pH 5.5 and 25 °C. Samples were taken at 5, 10, 15, 30, 45, 60, 75, 90, 105 and 120 min of contact time and analysed by ICP-OES to calculate the amount of removed Cu(II) (with same method discussed in section 2.4). Pseudo-first, pseudo-second and intraparticle diffusion models were used to understand the kinetics of the biosorption process.

2.7. Effect of biofilm incubation time on biosorption

Geotextile circles were harvested after 1, 7, 14, 21 and 28 days of incubation time in the bioreactor to investigate biosorption capacities and removal efficiencies of different stages of biofilm growth. Batch biosorption studies were carried out for 1, 5, 10, 20, 50, 100, 150 and 200 mg L^{-1} Cu(II) concentrations at pH 5.5 and 25 °C with 120 min contact time. Samples were taken from all days of biofilm incubation time and Cu(II) concentrations for ICP-OES analysis. The CFU plate count method (section 2.3) was used to evaluate toxicity of Cu(II) concentrations for bacterial colonies at different stages of biofilm development.

2.8. Control adsorption experiment

For all biosorption assays in this study, two sets of clean geotextile circles were washed thoroughly with ethanol to remove all living organisms on the surface of the geotextile and prevent any microbial growth, then soaked in two separate baths of deionized water and the same bioreactor medium without bacterial cultures for 28 days. The batch adsorption experiment was carried out for geotextiles without biofilm growth to measure possible Cu(II) removal by the geotextile fibres in contact with only water and oil.

2.9. FTIR analysis

Available functional groups on the biofilm before and after the biosorption process were analysed using Fourier Transform Infrared (FTIR) spectroscopy. Biofilms incubated for 28 days and 200 mg L^{-1} Cu(II) loaded biofilm were analysed by reflection FTIR with a cooled detector technique to analyse the absorption spectra of the bond in the range of 400–4000 cm^{-1}. The IR spectra before and after the biosorption process were compared to investigate the functional groups responsible for the Cu(II) removal. The FTIR instrument used in this study was a Nicolet iN10 Infrared Microscope (Thermo Fisher Scientific).

2.10. Experimental data modelling

All biosorption assays data were modelled using Langmuir (1916) and Freundlich (1906) isotherms. Intraparticle diffusion, pseudo-first and second equations were used to model kinetic of the biosorption. Finally, parameters such as ΔG, entropy (ΔS) and enthalpy (ΔH) were calculated for the thermodynamic model of the Cu(II) biosorption by the living biofilm.

2.11. Statistical analysis

All batch biosorption experiments in the present study were carried out using 20 replicates for each incubation time, pH, initial concentration, temperature and contact time. Although in most studies 3 replicates may be enough to carry out an accurate statistical analysis, the nature of living biofilm growth and uncertainties about microbial colonies convinced authors of this study to consider 20 replicates for all batch biosorption and CFU plate count assays.

3. Results and discussion

3.1. Equilibrium adsorption studies

3.1.1. Effect of pH on biosorption

An important factor in the biosorption process is pH as it influences the species distribution of the metal in solution as well as changing the association of functional groups present on the biofilm surface (Nederlof et al., 1993). Fig. 1. a illustrates Cu(II) biosorption capacities and removal efficiencies of by the living biofilm in different pH conditions. Prior to evaluating the effect of pH, it was important to understand the

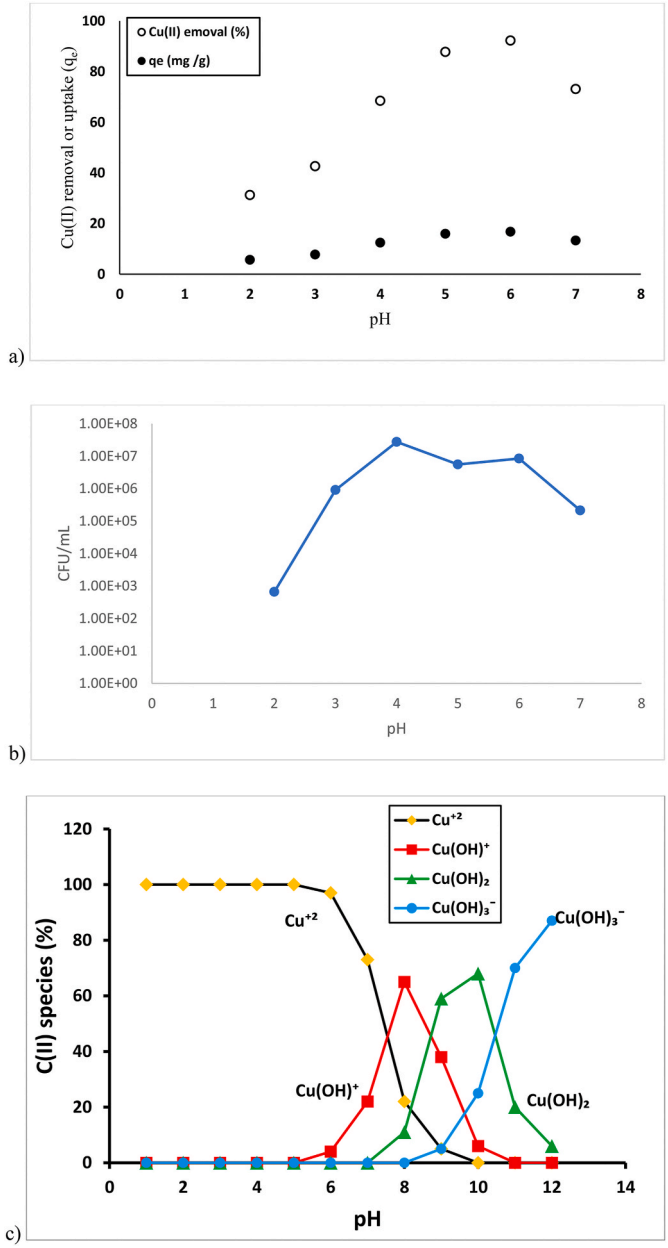

Fig. 1. a) Effect of pH on Cu(II) biosorption capacities and removal efficiencies of 7 days incubated geotextile circles at 25 °C and 120 min contact time. b) Effect of pH on colony count. c) Cu(II) species distribution as a function of pH at 25 °C.

predominant species of Cu(II) in accordance with the solution pH. Fig. 1c presents Cu(II) speciation of the solution at 25 °C with a Cu(II) ion content of 10 mg L^{-1}. The predominant species in different pH are as follows (El-Sheikh et al. 2018, 2019):

- At pH lower than 7.5, Cu^{2+} is the single predominant species of the solution.
- At pH between 7.5 and 8.5 the prominent species is $Cu(OH)^{+}$, where the Cu^{2+} concentration is dropping rapidly.
- Between pH 8.5 and 10.5, the concentration of $Cu(OH)^{+}$ is decreasing. However, at the same time $Cu(OH)_2$ species start to dominate the solution.
- At pH higher than 10.5 the predominate specie is $Cu(OH)_3^{-}$

In this study a pH between 2 and 7 was selected to investigate the effect of pH on biosorption of Cu(II) by the living biofilm. The reason for this selection was the predominance of Cu^{2+} in this pH range and as a result, there was less uncertainty about the effect of other Cu(II) species on the biosorption process. Moreover, Cu(II) precipitation was not observed at pH 2 to 7. According to Fig. 1a, the lowest biosorption efficiency (31%) and capacity (5.7 mg g^{-1}) was observed at pH 2. However, biosorption efficiency and capacity were increased by changing the pH from 2 to 6. The maximum biosorption efficiency (92%) and capacity (16.8 mg g^{-1}) was detected at pH 6. With increases in pH, the number of protons in the metal solution decreased. This phenomenon led to a lower proton competition with metal ions to bond with the functional groups available on the living biofilm surface. As a result, higher biosorption efficiencies and capacities were observed with the increase of pH. At pH 7, biosorption efficiency and capacity were 73% and 13.3 mg g^{-1}, respectively. As shown in Fig. 1c, at pH higher than 7 the predominance of Cu^{+2} in the solution decreased and large quantities of $Cu(OH)^{+}$ were present.

As it is described in section 3.4., the prominent functional group present on the living biofilm surface and associated with the Cu(II) biosorption process was the carboxyl group. At pH less than 3, the carboxyl group is in –COOH non-ionic form, which resulted in the lowest observed biosorption efficiencies and capacities at pH 2 and 3. This low efficiency was due to a lack of electrostatic interaction of –COOH non-ionic form of carboxyl groups with Cu(II) ions (Zhang et al., 2018). This observation revealed the role of electrostatic interactions in the Cu (II) biosorption process. However, with increases in pH to more than 3, the form of carboxyl group transformed from –COOH to -COO^{-} and accordingly, the Cu(II) removal efficiency and biosorption capacity were increased at pH 4 and 5 with the maximum occurring at pH 6. Previous studies in the literature have reported pH 6 as the optimum, with higher biosorption capacities (Choinska-Pulit et al., 2018; Letnik et al., 2017; Andreazza et al., 2010).

As pH is a crucial factor in bacterial survival (Wu et al., 2017), studying the effect of pH on colony forming unit counts (CFU) can provide valuable information on the environmental toxicity of urban runoff as well as biosorption studies (Griffiths and Philippot, 2013). The effect of pH on the colony count is shown in Fig. 1b. By increasing the pH from 2 to 4 the value of CFU per 1 mL of solution increased rapidly by five orders of magnitude. At pH 4 to 6 the value of CFU was approximately constant with less than 0.5-log change. However, the increase of pH from 6 to 7 resulted to a 2-log decrease in CFU per mL of solution, which may explain the decrease in biosorption efficiency between pH 6 and 7. By comparing Fig. 1a and b it can be observed that a living biofilm with more active and living bacteria was more efficient in Cu(II) removal, as a result of more bacterial metabolism, although the key explanation was the affinity between Cu(II) ions and the functional groups discussed earlier. It can be concluded that the change in functional groups available on the surface of the living biofilm can be observed as an indicator of a change in Cu(II) removal efficiency.

3.1.2. *Effect of Cu(II) initial concentrations on biosorption*

The initial metal ion concentration has a strong effect on the biosorption performance of bacterial strains (Kariuki et al., 2017). In order to determine the effect of Cu(II) initial ion concentrations on biosorption efficiencies and capacities of different stages of living biofilm, geotextile circles were harvested after 1, 7, 14, 21 and 28 days of incubation in the bioreactor.

The effect of the initial concentration (C_i) of Cu(II) on biosorption capacity (q_e) and removal efficiency (R) of different stages of biofilm growth, are illustrated in Fig. 2. a and Fig. 2. b, respectively. According to Fig. 2. a the biosorption capacity of all stages of biofilm growth increased as the initial concentration of Cu(II) increased. However, the opposite trend was observed for the removal efficiencies of all stages of biofilm growth (Fig. 2b), where removal efficiencies decreased with the increase of the initial concentrations. The maximum removal efficiency was for the biofilm on day 21 of growth with 97% removal for 1 mg L^{-1}

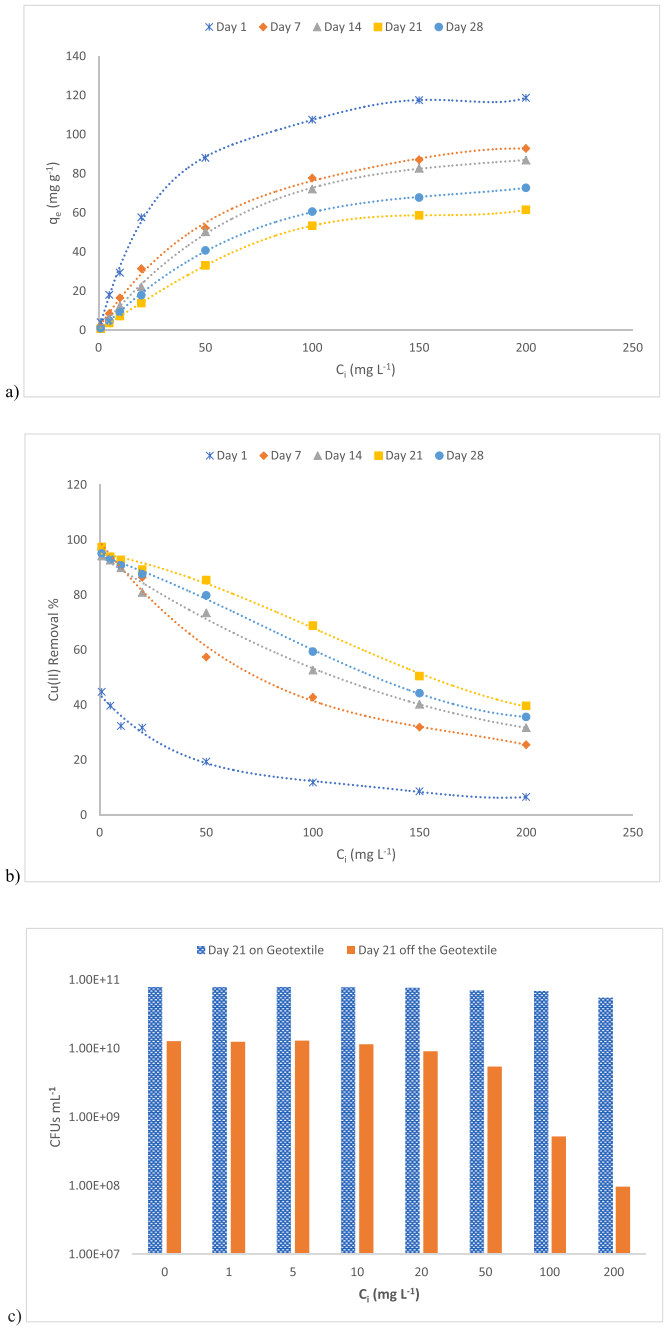

Fig. 2. The effect of initial Cu(II) concentration on a) biosorption capacity, b) removal efficiency and c) CFU mL^{-1} of the living biofilm on and detached from the geotextile at pH 5.5 and 25 °C for 120 min contact time.

initial concentration. The minimum removal efficiency (7%) was associated to geotextiles on day 1 of biofilm growth for 200 mg L^{-1} initial concentration. However, the maximum removal efficiency for 200 mg L^{-1} was observed in sample from day 21 with 40% metal removal. With lower initial concentrations the biosorption efficiencies showed higher values. The maximum efficiencies for 150, 100 and 50 mg L^{-1} initial concentrations were 50%, 68% and 85%, respectively. This increase in efficiencies continued at 20, 10, 5 and 1 mg L^{-1} initial concentrations with maxima of 89%, 93%, 94% and 97% Cu(II) removal, respectively. The observed decrease in efficiencies with the increase of initial concentrations can be explained by the fact that by increasing the concentrations of Cu(II), the number of ions competing for binding with functional groups available on the biofilm, increased. Therefore, more Cu(II) ions were left in the metal solution and as a result, lower removal efficiencies were observed (Ucun et al., 2009). As illustrated in Fig. 2b, different stages of biofilm growth showed removal efficiency of more than 60% difference and this difference was greater with higher concentrations of Cu(II). This result is discussed in detail in section 3.1.4 regarding the effect of living biofilm incubation time on biosorption capacities.

Fig. 2a shows the biosorption capacity of different stages of biofilm development as a function of initial concentration. The biosorption capacity of all stages of biofilm development increased with the increase of initial Cu(II) concentration. The increase of biosorption capacity with the increase of initial concentration was due to the higher availability of Cu(II) ions in the solution to bond with the available biosorption sites on the biofilm surface. Higher concentrations of Cu(II) resulted in a greater gradient of ion concentrations that increased the chance of Cu(II) ions colliding with the functional groups of living biofilm and consequently a higher Cu(II) biosorption capacity (Shroff and Vaidya, 2011; Suazo--Madrid et al., 2011). The maximum biosorption capacity (119 mg g^{-1}) was observed in samples from day 1 of incubation time with the initial concentration of 200 mg L^{-1} and the least biosorption capacity was associated with day 21 of incubation time and 1 mg L^{-1} initial concentration. This observation was contrary to the removal efficiency, where the maximum removal efficiency occurred at 1 mg L^{-1} initial concentration and day 21 incubation time. The reason for this observation is discussed in section 3.1.4.

Bacterial colonies have a crucial role in nutrient cycling in soil and water. Moreover, bacteria are the nutrient source for microorganisms higher in the food chain. In order to achieve a sustainable and healthy soil and aquatic ecosystems, it is important to understand how and to what extent soluble metals in runoff can alter microbial life. Fig. 2c illustrates the toxicity of different concentrations of Cu(II) to bacterial biofilm on and off the geotextile at pH 5.5 and 25 °C. According to this figure, CFU mL^{-1} of samples exposed to Cu(II) concentrations on geotextile altered significantly less than samples taken from off geotextile treatments. Biofilms from the geotextile showed 1.2-log and 2-log decreases after exposure to 150 and 200 mg L^{-1} Cu(II), respectively. However, unaltered biofilms on geotextile circles showed less than 0.2-log decrease at the same toxicity test conditions. This indicated the importance of living biofilm and geotextile within the structure of porous pavements, that not only did 21 days of biofilm incubation on a geotextile decrease the Cu(II) concentration between 40% and 97% (depending on the metal concentration), but also protected 100 times more bacteria that are crucial for biosorption and a healthy ecosystem. The biofilm protects the bacteria through two main mechanisms. The initial resistance layer of the biofilm is known as glycocalyx with a thickness between 0.2 and 1.0 μm (Flemming and Wingender, 2001). The glycocalyx matrix is made of glycoprotein and polysaccharides and uses electrostatic, Van Der Waal and hydrogen bonds forces to adhere biofilm to the surfaces (Peña et al., 2011). The flexible glycocalyx layer accumulates heavy metals ions up to 25% of its weight and through this mechanism protects the bacteria (Singh et al., 2017). The second mechanism of protection against Cu(II) ions is by detoxification which occurs through enzymatic reduction of metal resistance genes and copper ions (Tapiero et al., 2003).

3.1.3. Modelling of equilibrium biosorption data

Adsorption isotherms help with an understanding of the affinity and distribution of adsorbate bonding sites between two separate phases of metal solution and an adsorbent surface (Kyzas and Matis, 2015). Modelling of equilibrium adsorption data reveals information about the mechanism, process and metal-adsorbent affinity of the biosorption experiment. Langmuir and Freundlich adsorption models were used to evaluate the Cu(II) biosorption data. The Langmuir isotherm (1916) assumes the adsorbent surface as a homogeneous site where adsorption takes place and is expressed by:

$$\frac{C_e}{q_e} = \frac{C_e}{q_{max}} + \frac{1}{q_{max} K_L}$$

where q_e is the amount of Cu(II) adsorbed at the equilibrium (mg g^{-1}), C_e is the concentration of Cu(II) in the solution at the equilibrium (mg L^{-1}), q_{max} is the maximum monolayer biosorption capacity of the biofilm (mg g^{-1}) and K_L is the Langmuir constant (L mg^{-1}). In order to calculate K_L and q_{max}, C_e/q_eshould be plotted against C_e where the slope and intercept of resulted straight line are $1/(q_{max}K_L)$ and $1/\ q_{max}$, respectively.

The Freundlich isotherm (1906), unlike the Langmuir isotherm that assumes a monolayer of adsorbed molecules, considers multi-layer adsorption sites and is expressed by:

$$\log q_e = \left(\frac{1}{n}\right) \log C_e + \log K_F$$

where is the amount of Cu(II) adsorbed at the equilibrium (mg g^{-1}), C_e is the concentration of Cu(II) in the solution at equilibrium (mg L^{-1}), K_F and n are biosorption extension and nonlinearity indicators that are calculated by plotting log q_e vs log C_e, where the slope and intercept of the resulting graph are $1/n$ and log K, respectively. The n-value indicates whether the adsorption process is favourable under the conditions in the study.

The equilibrium biosorption of Cu(II) by different stages of the living biofilm growth at pH 5.5 and 25 °C, was modelled by plotting q_e against C_e and are shown in Fig. 3. Langmuir and Freundlich isotherms were used for the biosorption data, linear correlation coefficient (R^2) and isotherm constants were calculated and are presented in Table 1 and Figure SI2. The high values of R^2 (0.991–0.999) in the Langmuir isotherm indicated the monolayer adsorption nature of the biosorption of Cu(II) by all stages of the biofilm growth. R^2 values are slighter lower (0.942–0.964) for the Freundlich isotherm, which revealed that biosorption was not onto a multilayer of biofilm, but rather on a monolayer uniform site. However, multilayer biosorption had an additional role in Cu(II) removal by the living biofilm. According to Fig. 3 and Table 1 the maximum biosorption capacity (132 mg g^{-1}) of the living biofilm occurred on geotextile harvested on day 1. This observation confirmed the monolayer adsorption nature of the biofilm as on day 1 of biofilm growth, as there were less layers of bacteria grown on the geotextile surface and as a result the proportion of surface to mass is the lowest in comparison to later stages of biofilm growth. Thus, day 1 showed the maximum biosorption capacity and this value decreased as the biofilm was developed and added more layers. As discussed in section 3.1.2, the highest biosorption capacity did not necessarily lead to the highest removal efficiency (day 1 showed the lowest efficiency).

Table 1
Adsorption constants of Langmuir, Freundlich isotherms.

	Langmuir Model			Freundlich Model			Isotherm shape
	Q_{max} (mg g^{-1})	K_L (L mg^{-1})	R^2	K_F	N	R^2	
Day 1	132	0.052	0.999	8.6	1.77	0.942	L-2
Day 7	94	0.15	0.991	12.74	2.23	0.955	L-2
Day 14	91	0.12	0.996	9.2	1.90	0.961	L-2
Day 21	64	0.18	0.999	7.3	1.88	0.964	L-2
Day 28	75	0.14	0.998	7.8	1.86	0.955	L-2

All stages of biofilm growth shown an L2 isotherm shape (Fig. 3 and Table 1) according to the Giles classification (Giles and Smith, 1974). The L2 shape revealed that Cu(II) biosorption took place on a monolayer on the living biofilm surface (Giles and Smith, 1974). Furthermore, the L2 shape of isotherms in all days was associated with a high affinity between Cu(II) ions in the solution and the living biofilm surface at lower concentrations. Therefore, the biofilm surface was saturated at higher concentrations and as a result showed lower efficiencies (see section 3.1.2).

3.1.4. *Effect of incubation time on biosorption capacity of living biofilm*

Living biofilms are dynamic communities of microorganisms, therefore biofilm properties are constantly changing and as a result, the biosorption behaviour of the living biofilm may be subject to change. In order to evaluate this change, geotextile circles incubated for 1, 7, 14, 21 and 28 days in the bioreactor were harvested prior to biosorption experiments, using the same method described in section 3.1.2. The effect of biofilm incubation time on biosorption of different concentrations of Cu(II) is illustrated in Fig. 4. a. For all concentrations of Cu(II), biofilms with 1 day of incubation time, showed the highest biosorption capacities ranging from 4 to 119 mg g^{-1} for 1 and 200 mg L^{-1} Cu(II) concentration, respectively. The biosorption capacity reduced as the biofilm developed, where the minimum biosorption capacities occurred on day 21 of the incubation time with a biosorption capacity ranging between 0.75 and 61 mg g^{-1}. However, as discussed in section 3.1.2, removal efficiencies of different stages of biofilm growth had a different trend where minimum removal efficiency was observed on day 1 and the maximum occurred on day 21 (Fig. 2b). The reduction of biosorption capacity

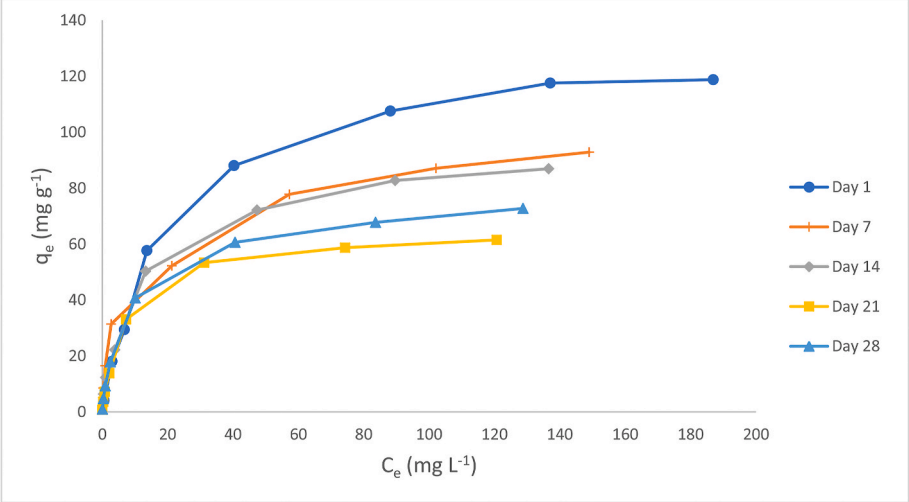

Fig. 3. Modelling of equilibrium Cu(II) biosorption (q_e vs. C_e) for different stages of biofilms at pH 5.5, 25 °C.

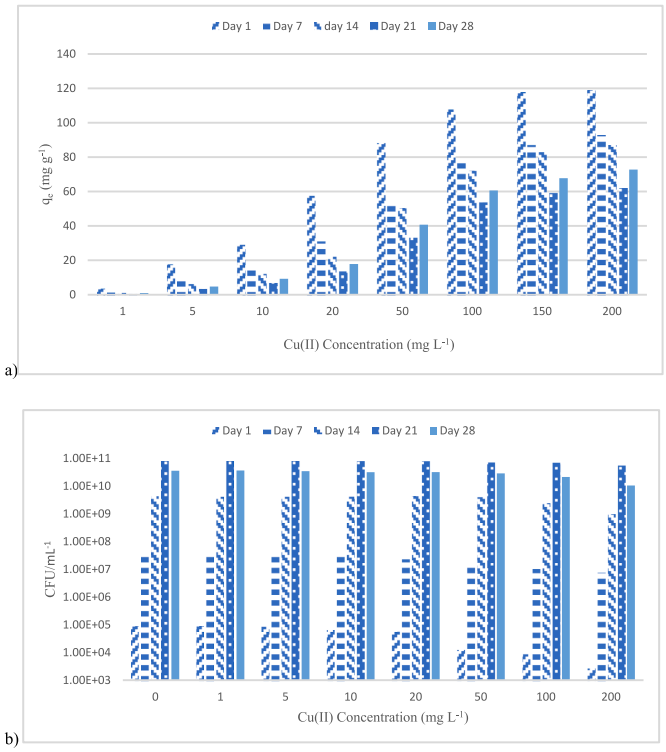

Fig. 4. a) Effect of incubation time on the living biofilm capacity at pH 5.5 and 25 °C and 120 min contact time. b) Toxicity of different concentrations of Cu(II) on bacterial communities on different stages of biofilm development at pH 5.5 and 25 °C and 120 min contact time.

between day 1 and 21 was due to the fact that a monolayer was responsible for the biosorption of Cu(II) (see section 3.1.3). Therefore, by increasing the incubation time, the biofilm mass increased but the inner layers were less active in the biosorption process. Although more biosorption surface was available, leading to higher removal efficiency, less biosorption surface to mass ratio was available for biosorption. However, the biosorption capacity increased between day 21 and 28 for all Cu(II) concentrations (Fig. 4a). The reason for this increase was the dispersion stage of the biofilm development where some parts of the biofilm were detached and released in the bioreactor solution (Guilhen et al., 2017). The mass (used for biosorption capacity calculations) of biofilms on geotextiles harvested on day 28 showed less mass than day 21 and suggested that the dispersion stage happened between day 21 and 28 (due to a higher q_{max} for day 28 in Table 1).

Incubation time had a significant effect on the removal efficiency and biosorption capacity of the biofilm where in more developed biofilms, maximum removal efficiency and minimum biosorption capacity occurred simultaneously due to the monolayer adsorption facilitation of the process.

In order to evaluate the toxicity of Cu(II) ions to the bacterial communities, geotextile circles were harvested at different stages of the biofilm growth prior to their exposure to 1–200 mg L^{-1} Cu(II) concentration for 120 min at pH 5.5 and 25 °C. The geotextile circles were agitated in 10 mL of deionized water to disperse the bacteria into the solution. A 1 mL sample of each treatment was serially diluted and plated for the CFU count. Fig. 4b shows the toxicity of different concentrations of Cu(II) ions to the bacterial communities on biofilm with different incubation times. According to control values in Fig. 4b, CFUs increased by 6 orders of magnitude, from day 1 to day 21, and this indicated the development of the biofilm. However, a decrease was observed between day 21 and 28 where the dispersion stage of the biofilm development may have occurred. This observation might address the removal efficiency increase between day 21 and 28 (Fig. 4a).

According to Fig. 4b, CFUs decreased from 5.50 x 10^{10} to 3.04 x 10^{8} where exposed to 200 mg L^{-1} Cu(II) on day 1. However, the toxicity of high concentrations of Cu(II) decreased as the biofilm developed and led to a less than 0.1 log unit decrease on day 21 compared with the control. This observation can be associated with development of Extracellular Polymeric substances (EPSs) that have a protection effect and shield the bacterial communities (Costa et al., 2018; Yin et al., 2019). This protection was reduced between day 21–28 where the dispersion stage of biofilm development occurred and as result, a reduction in CFUs was observed. Possible EPS protection was also observed in Fig. 2c where Cu (II) ions showed more toxicity to bacteria when removed from the geotextile in comparison with bacterial communities inside the EPS coat. This experiment indicated the efficiency of geotextile biofilms in Cu(II) removal and the resistance of biofilm organisms to the toxicity of Cu(II).

3.2. Thermodynamics of biosorption: effect of temperature

Thermodynamic studies were carried out by varying the biosorption temperature between 25 and 55 °C. Geotextile circles with 7 days incubation time were harvested prior to the biosorption experiment (with the same method described in section 3.1.1) at pH 5.5 with 4 different temperatures (25, 35, 45 and 55 °C). The biosorption equilibrium (q_e) versus equilibrium concentration (C_e) of Cu(II) removal by biofilm, at temperatures between 25 and 55 °C are shown in Fig. 5. According to this figure, the value of q_e increased with increase of temperature from 25 to 35 °C and the maximum q_e occurred at 35 °C. The maximum biosorption of metals by the living mixed culture of bacteria, occurring at temperatures between 32 and 35 °C have been reported previously by researchers (Taragini and Satpathy 2009; Alpat et al., 2010). This could be due to the structure of EPS at 35 °C, that has been reported to be the optimum temperature for EPS production (Arun, 2014). However, by increasing the temperature from 35 to 55 °C, the q_e value decreased from 116 to 74 mg g^{-1}. The observed decrease in biosorption at higher temperatures may be due to the formation of metal-biofilm complexes and the instability of biofilm at high temperatures and as a result the metal removal from the biofilm surface. Furthermore, high temperatures can damage the active binding sites available on the surface of the biofilm resulting to lower biosorption of Cu(II) at higher temperatures.

Thermodynamic parameters including **Δ**G, entropy (ΔS) and enthalpy (ΔH) were calculated using Gibbs free energy change as expressed below (El-Sheikh et al., 2011; El-Sheikh 2014):

$$K = Q_{\max} K_L$$

$$\Delta G = RT \ln K$$

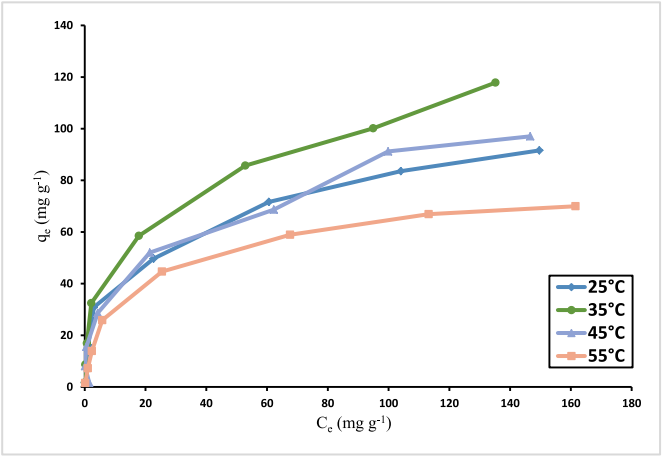

Fig. 5. Effect of temperature for 7 days incubated biofilms at pH 5.5 and 120 min contact time.

$$\Delta G = \Delta H - T \cdot \Delta S$$

where ΔG (J mol^{-1}) is Gibb's free energy change for the biosorption, T is the temperature in Kelvin, R is the universal gas constant (8.314 J mol^{-1} K^{-1}), K is an equilibrium constant. A plot of ΔG against T will provide a linear plot and values of -ΔS and ΔH are slope and intercept, respectively.

Thermodynamic parameters were calculated for all temperatures and are presented in Table 2. The ΔG values were negative (−5.099 to −6.735) for the biosorption at all temperatures, that indicated the feasibility of spontaneous Cu(II) removal by the living biofilm at all the studied temperatures (Das and Dash 2017). However, the ΔG value became less negative at higher temperatures, and predicted the decrease in degree of spontaneity and favourability at higher temperatures (O'Hayre 2014). The ΔG values were in the range of 0 to −20 $kJmol^{-1}$ for all temperatures, showing that the Cu(II) removal by the biofilm was a physisorption process (Erkey, 2011). Moreover, the negative value of entropy (ΔS = −54.8) revealed the decrease in degrees of freedom and randomness of the adsorbed metal ions on the surface of living biofilm (Ben-Tal et al., 2000). Finally, the negative value of enthalpy (ΔH = −23.2) indicated the exothermic nature of the biosorption process. As a conclusion, thermodynamic parameters suggested that the Cu(II) biosorption by the living biofilm was of a physical nature, feasible, spontaneous and exothermic under these research conditions.

3.3. Kinetics of biosorption

Batch kinetic studies were carried out to investigate the effect of contact time on Cu(II) biosorption by the living biofilm and provide information on rate controlling processes. Geotextile circles were harvested on day 7 of incubation in the bioreactor prior to being exposed to 1, 5, 10, 20, 50, 100, 150 and 200 mg L^{-1} Cu(II) concentrations at pH 5.5 and 25 °C. The amount of metal adsorbed per unit of mass was calculated at 5, 10, 15, 30, 45, 60, 75, 90, 105 and 120 min of contact time. The results of the experiment and kinetics of biosorption modelling are presented in Fig. 6. According to this figure, at lower concentrations of Cu(II) ions (less than 50 mg L^{-1}), the metal solution reached equilibrium in less than 15 min of contact time. However, at higher concentrations of Cu(II) (100–200 mg L^{-1}) the equilibrium occurred after 45 min of contact time.

Two main models used for modelling the kinetics of biosorption are pseudo-first and pseudo-second equations (Xu et al., 2004). The pseudo-first order equation (Lagergren, 1898), that assumes linear driving force, is as follows:

$$\frac{dq_e}{dt} = k_1(q_e - q_t)$$

where q_e (mg g^{-1}) is the biosorption capacity at equilibrium, q_t (mg g^{-1}) is the biosorption capacity at time t, and k_1 is model constant (min^{-1}). The equation to calculate thek_1 value is as follows:

$$\log\left(\frac{q_e - q_t}{q_e}\right) = -\frac{k_1}{2.303}t$$

where k_1 is slope of the plotted line of $\log((q_e - q_t)/q_e)$against t.

The pseudo-second order kinetic was offered Blanchard et al. (1984). However, Ho and McKay, (1998) reviewed the equation and proposed the following:

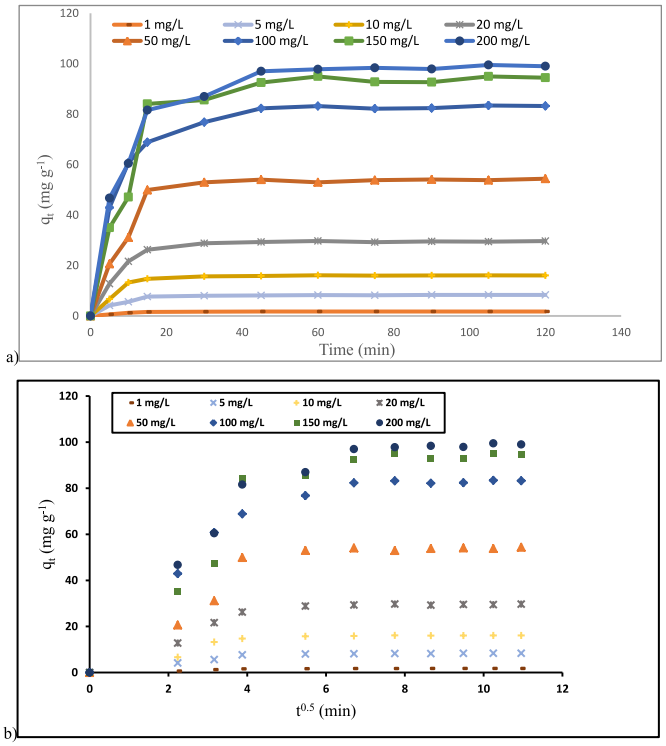

Fig. 6. a) Effect of initial Cu(II) concentration and contact time on Cu(II) biosorption by 7 days incubated living biofilm at pH 5.5, 25 °C. b) Intra-particle diffusion model of the Cu(II) biosorption process.

$$\frac{dq_t}{dt} = k_2(q_e - q_t)^2$$

where k_2 (g mg^{-1} min^{-1}) is the pseudo-second equation constant and is calculated by:

$$\frac{t}{q_t} = \frac{1}{h} + \frac{1}{q_e}t$$

$$h = k_2 q_e^{\ 2}$$

where h (mg g^{-1} min^{-1}) is the biosorption rate, q_e and $k_2$are slope and intercept of the line plotted by tq_t against t, respectively.

Pseudo-first-order and pseudo-second-order adsorption rate constants, were applied and the experimental biosorption capacities for living biofilms incubated for 7 days, with different concentrations of Cu (II) are presented in Table 3. According to the table, the R^2 values in the pseudo-second order model are higher than pseudo-first order at all Cu (II) concentration. Thus, the experimental data followed the pseudo-second order kinetic model, that indicated the rate controlling nature and significant contribution of diffusion in the external layer of the living biofilm in the Cu(II) biosorption process (He et al., 2015; Simonin and Boute, 2016; Russo et al., 2016; El-Sheikh 2014; El-Sheikh et al., 2011).

Table 2
Thermodynamic parameters for biosorption of Cu(II) by living biofilm at pH 5.5

T (kelvin)	Q_{max}	K_L	R^2	K	ln K	ΔG (kJ mol^{-1})	ΔH (kJ mol^{-1})	ΔS(J K^{-1} mol^{-1})
298	94	0.15	0.991	14.1	2.65	−6.565	−23.2	−54.8
308	116	0.12	0.9784	13.9	2.63	−6.735		
318	100	0.085	0.9785	8.5	2.14	−5.658		
328	74	0.088	0.9969	6.5	1.87	−5.099		

Table 3
Comparison of pseudo-first-order and pseudo-second-order adsorption rate constants, calculated and experimental Cu(II) biosorption capacities of 7 days incubated living biofilm at pH 5.5 and 25 °C.

	1 mg L^{-1}	5 mg L^{-1}	10 mg L^{-1}	20 mg L^{-1}	50 mg L^{-1}	100 mg L^{-1}	150 mg L^{-1}	200 mg L^{-1}
$q_{e,exp}$ (mg g^{-1})	3	10	18	31	58	87	100	105
Pseudo-1st order								
R^2	0.5177	0.5854	0.5620	0.6617	0.6667	0.7853	0.7627	0.8865
Pseudo-2nd order								
R^2	0.9969	0.9987	0.9981	0.9983	0.9960	0.9990	0.9947	0.9981
$q_{e,cal}$ (mg g^{-1})	1.8	8.6	16.4	30.5	56.5	85.5	99.0	103.1
k_2(g $mg^{-1}min^{-1}$)	0.16	0.042	0.025	0.012	0.0045	0.0040	0.00002	0.0024

3.3.1. Intraparticle diffusion

Langmuir, Freundlich, Pseudo-first and second models do not take diffusion into account (Majumdar et al., 2016). Film diffusion (external mass transfer), pore diffusion (intraparticle pore diffusion) or both processes may control the biosorption process and the slower one is the rate limiting step (El-Sheikh 2014; Baraka, 2015;). The Weber and Morris (1963) intra-particle diffusion model was used to evaluate the kinetic experimental data and obtain more information about the diffusion processes controlling the Cu(II) biosorption by the living biofilm. This model assumes that intraparticle diffusion is the rate controlling stage in the biosorption process. The Weber and Morris intraparticle diffusion equation is:

$$q_t = k_{id} t^{0.5} + C$$

where k_{id} (mg $g^{-1/2}$ $min^{-1/2}$) is the intraparticle diffusion rate constant and C is the diffusion boundary layer thickness constant. Fig. 6b illustrates the intra-particle diffusion model of the Cu(II) biosorption process by the biofilm. The shape of graphs for different initial concentrations revealed the mechanism of the biosorption process.

According to Fig. 6b, During biosorption of low concentrations of Cu (II) (less than 50 mg L^{-1}) intraparticle diffusion occurred between $t^{0.5}$ values of 0 and 4 as there was only one straight line passing through the origin. This observation revealed that for concentrations less than 50 mg L^{-1} the biosorption process occurred with a single stage intraparticle diffusion and was the rate-limiting stage before reaching the equilibrium concentration. However, for higher concentrations of Cu(II) (100–200 mg L^{-1}) a biphasic (two linear lines) plot was observed. The first line between $t^{0.5}$ values of 0 and 4 with a steeper slope indicated that film diffusion (surface biosorption) was the rate limiting step and around 80% of the final biosorption capacity was occupied by the Cu(II) ions. However, the second rate-limiting step with $t^{0.5}$ value between 4 and 5.5 was observed, where the line with lower slope was an indication of the pore diffusion (intra-particle diffusion) process and reached the maximum biosorption at $t^{0.5}$ value of 7. The second line that represented the intraparticle diffusion can be explained by higher concentration of Cu(II) that pushed the metal ions to inner layers of the living biofilm and as a result showed a higher biosorption capacity at higher concentrations. This observation could explain the 0.5 log reduction in CFUs count at higher Cu(II) concentrations on day 7 (Fig. 4b), that can be due to the second rate-limiting intraparticle diffusion stage of the biosorption observed in Fig. 6b where protective EPS layer became saturated with Cu(II) ions. However, the EPS showed a better efficiency in protecting the bacteria at lower concentrations due to the lower ion pressure and lack of intraparticle diffusion stage.

3.4. IR study: mechanism of Cu(II) biosorption on living biofilm

Functional groups on the active sites of the biofilm are considered as biosorption agents responsible for metal removal from solutions (Kapoor and Viraraghavan, 1997). IR spectra of 28 days incubated biofilm before and after binding with 200 mg L^{-1} Cu(II) ions at pH 5.5 and 25 °C, was carried out for identification of functional groups on the biofilm and their contribution in the biosorption process. The IR spectra of Cu(II) loaded and unloaded biofilm in the range of 700–4000 cm^{-1} is shown in Fig. 7.

According to the IR spectra before binding with metal in Fig. 7, the bands in the range of 3200–3400 cm^{-1} were assigned to O–H and N–H bands of hydroxyl and amine groups. The bands between 2910 and 2930 cm^{-1} were an indication of the presence of C–H bands of alkane groups. The peak observed in the range of 1710–1740 cm^{-1} was recognized as C═O stretching in the carbonyl group. Stretching appeared between 1540 and 1550 cm^{-1} and this was an indication of COO- bands of carboxyl groups. Furthermore, –COOH bands of carboxyl groups appeared at 1390 cm^{-1} and the peak at 1238 cm^{-1} was assigned to C═O stretching of carboxyl groups. Finally, P–O bands of phosphate groups appeared between 1070 and 1075 cm^{-1}. Changes in IR spectra after Cu(II) ions loading were as follows:

A 30 cm^{-1} shift and broadening of the spectra was observed at 3270 cm^{-1} after the metal loading, that indicated the possibility of binding between N–H bands of primary amines available on the biofilm surface and Cu(II) ions. The IR spectra after the biosorption revealed the stretching and shifting of the bands between 1710 and 1720 cm^{-1}, that could be due to the involvement of C═O bands of carbonyl groups in the Cu(II) biosorption process. The increase, shifting by10 cm^{-1}, and broadening of the peak at 1390 cm^{-1} was an indication of a considerable contribution of –COOH bands of carboxyl groups available on the biofilm in the Cu(II) complexation and removal process. Higher absorbance behaviour of the biofilm at bands between 1235 and 1238 cm^{-1} and also shifting of the IR spectra was attributed to C═O stretching of carboxyl groups and their interaction with Cu(II) ions. The occupation of carboxyl groups by Cu(II) ions resulted in the observed higher absorbance of the biofilm after the binding process. Likewise, the shift and higher absorbance in IR spectra at 1075 cm^{-1} verified the interaction between Cu(II) ions and P–O bands of phosphate groups during the biosorption process.

FTIR analysis indicated that carboxyl, hydroxyl, amino and phosphate groups were the most important contributors in the Cu(II) ions

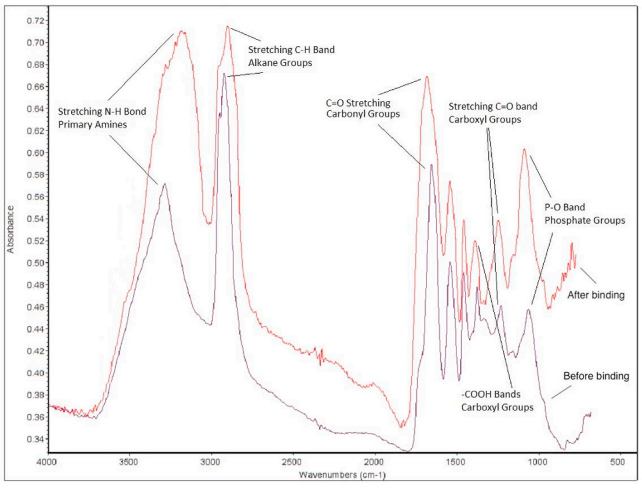

Fig. 7. The IR spectra of 28 days incubated biofilm before and after binding with 200 mg L^{-1} Cu(II) ions for 120 min at pH 5.5 and 25 °C.

complexation, binding and removal by the living biofilm. These functional groups have been reported by various previous studies as the main biosorption agents (Giotta et al., 2011; Huang et al., 2013; Xia et al., 2015; Yang et al., 2017; Fathollahi et al., 2020b).

3.5. Control adsorption experiment

As discussed in section 3.1.2 the living biofilm incubated for 28 days, showed removal efficiencies between 36% and 95% for initial concentrations of 200 and 1 mg L^{-1}, respectively. It was necessary to carry out a control batch adsorption experiment to measure the removal efficiency of the geotextile used in this study without a biofilm layer involved. The control study was intended to indicate the validity of the main study and determine the contribution of clean geotextile fibres in the Cu(II) removal process. Two sets of 20 geotextile circles were washed thoroughly with detergent to remove all dust prior to soaking in 94% ethanol solution to remove all living organism on the surface of the geotextile to prevent any microbial growth. The first set of the geotextiles were incubated in deionized water for 28 days. The second set of the geotextiles were soaked in a solution with the same medium as the original bioreactor, with no microbial culture to prevent the biofilm growth. This control experiment was designed to investigate the possible effect of water and other ingredients on geotextile fibres after 28 days and any increase in the adsorption of Cu(II) efficiencies. Both sets of control geotextile circles were harvested after 28 days prior to the batch adsorption experiments with the same procedure discussed in section 3.1.2. The results of ICP-OES analysis showed removal efficiencies of near 0% (below ICP-OES instrumentation detection limit) for all concentrations of Cu(II) (1–200 mg L^{-1}) at pH 5.5 and 25 °C. This observation indicated the overwhelming role of the living biofilm in biosorption of Cu(II) ions from solution. This is in line with FTIR results that indicated the involvement of carboxyl, hydroxyl, amino and phosphate functional groups available on the surface of the biofilm in the biosorption process.

3.6. Comparison of different stages of living biofilm with other biosorbents

Table 3 compares the maximum Cu(II) biosorption capacities of the living biofilm with different lengths of incubation time, against other biosorbents in the literature. All stages of the biofilm growth showed higher Cu(II) biosorption capacities when compared with other reported research values. However, a direct comparison was not feasible as experimental methods including initial concentrations, initial biosorbent dose, contact time, temperature and pH were different.

3.7. Implications for stormwater water quality improvements

As shown in Table 4, mixed bacterial communities present on a geotextile as a biofilm, perform well in comparison with other biosorbent materials. The research in this was report was deliberately simplified in order to chemically describe the processes of biosorption, but the current study differs from other reports of microbial biosorption (e.g. Chen et al., 2005; Choudhary and Sar, 2009; Cerino-Córdova et al., 2012) in that the microbial communities in the present study were not a single species. Like Chen et al., 2005, the biofilm in our studies used living microbes, which have better biosorption performance than non-living biomass. One reason that a living multi-species biofilm performs well against chemical challenge, is that the microbes are embedded in extracellular polymeric substances (EPS) which is thought to both protect the biofilm, ensure hydration and to participate in the biosorption process. The relatively small impact of 200 mg/L-1 of Cu(II) on the survival of biofilm bacteria relative to controls with no Cu(II) as described in this study, provides evidence of a biosorption process that is not necessarily harmful to the organisms that are involved. It was observed that once the biofilm was detached from the growth platform and not in the EPS on the geotextile, the survival of bacteria after interaction with Cu(II), measured by colony forming units, was much reduced. It will be important to examine more complex developed biofilms for their efficacy against dissolved metals and this work is underway (Coupe et al. in preparation). Larger scale more developed biologically active stormwater systems have variable relations with dissolved metals. Bioretention systems with compost as the source of organic material, intended to prevent the export of dissolved metals, facilitated copper export in the early life of the drainage system, and complexing with dissolved organic matter DOM. This copper/DOM complex was considered less toxic than free copper ions and later in the life of the system, (after the first 3-5 storms) the bioretention system became a sink for copper (Chahal et al., 2016).

LaBarre et al. (2016) examined the interactions between runoff from copper clad roofs and bioretention swales and planter boxes positioned to receive the runoff. The performance of both types of stormwater control measure (SCM) was effective, in reducing both the concentration of released copper, measured at 2.16 g/m^2/year and the attenuation, which had median values of 94% in the planters and 99% in the swales. LaBarre et al. did not explore the retention mechanisms for Cu in the SCM, either the complexing of Cu with the compost amended native soil used as growth medium, or the role of the biological factors that contributed to the attenuation performance.

Liu et al. (2019) examined the removal of copper in the layers of laboratory scale permeable pavements and showed that depth of pavement, smaller aggregate sizes and lower rainfall intensities correlated with better copper removal efficiencies, but despite the presence of a geotextile in the designs, there was no examination of the performance of the geotextile layer in sorption of copper, nor the likelihood of the role of microbes in the processes of attenuation. Many of the added model pollutants were likely to sustain microbiological life (organic impurities in TSS, phosphorus, nitrogen) and as noted by Liu et al., NH4–N is trapped successfully by adsorbents, in this case kaolin, but equally NH4–N could be utilised in microbial processes. Nitrogen is an important macronutrient and NH4–N could be susceptible to ammonia-oxidising bacteria (AOB), generating nitrite-nitrogen (NO −-N), (Maharjan. et al., 2020), generating biomass and adding to biosorption totals. Bradley et al. (2012) examined the removal of copper by permeable friction course (PFC), which is an asphalt based shallow permeable pavement type that decreased the Cu in effluent by 60% relative to conventional impermeable highway surfacing material.

None of the studies cited above focused specifically on the environmental challenge of dissolved copper in stormwater or examined the

Table 4
Comparison of biosorption capacities of different stages of living biofilm growth for Cu(II) with other biosorbents.

Biosorbent	Maximum Cu(II) adsorption capacity(mg L^{-1})	References
1 day incubated living biofilm	119	Current study
7 days incubated living biofilm	92	Current study
14 days incubated living biofilm	86	Current study
21 days incubated living biofilm	61	Current study
28 days incubated living biofilm	72	Current study
Bacterial cellulose	24	Jin et al. (2017)
Sophora japonica pods	35	Amer et al. (2015)
Carbonized medlar-core	43	Langroodi and Safaei, 2016
Watermelon shell	31	Gupta and Gogate (2016)
Arachis hypagaea husk	14	Ingle et al. (2015)
Sawdust	4	Putra et al. (2014)
Eggshell	34	Putra et al. (2014)
Sugarcane bagasse	4	Putra et al. (2014)

biological properties of biofilm for biosorption. Despite the great potential shown in the performance of early growth biofilm on a common building material such as Inbitex, attention must now focus on the longer-term performance of living microbe biosorption, the impact of other chemicals on the process, dehydration of the biomass, temperature and whether biological processes may inhibit the biosorption process, for example by bacterial competition or predatory behaviour by protists.

4. Conclusions

This study reports the impact of initial metal concentrations, contact time, temperature and pH on living biofilm equilibrium, thermodynamics and kinetics of Cu (II) biosorption. Moreover, the toxicity of different concentrations of Cu(II) and pH on CFU number in different stages of biofilm growth was carried out. FTIR analysis was conducted to evaluate functional groups responsible for the Cu(II) removal. Langmuir and Freundlich isotherms were used to model the equilibrium biosorption data.

The maximum CFU number was observed on day 21 of incubation time where the maximum resistance against 200 mg L^{-1} Cu(II) was observed that was due to a more developed EPS protection layer. The maximum biosorption capacity was measured on day 1 of incubation time, however the maximum removal efficiency (97%) was observed on day 21 of biofilm growth. According to the thermodynamics parameters, Cu(II) biosorption by the living biofilm had a physical nature and was exothermic, feasible and spontaneous. Kinetic of the biosorption indicated that the diffusion in external layer of the biofilm controlled the biosorption process in lower concentrations of Cu(II). However, in higher concentrations a combination of film and intraparticle diffusion took place and fitted pseudo-second order model. Modelling of the equilibrium data revealed that a monolayer on the living biofilm surface was active in the metal binding process. FTIR analysis identified carboxyl, hydroxyl, amino and phosphate groups as the functional groups that contributed in Cu(II) ions complexation by the living biofilm.

Author Statement

Alireza Fathollahi, Conceptualization, Methodology, Validation, Formal analysis, Investigation, Resources, Writing – original draft, Writing – review & editing. Stephen J Coupe, Conceptualization, Methodology, Validation, Investigation, Resources, Writing – original draft, Writing – review & editing, Supervision, Project administration. Amjad H. El-Sheikh, Methodology, Validation, Writing – original draft, Writing – review & editing. Ernest O Nnadi, Writing – original draft, Writing – review & editing

Declaration of competing interest

The authors declare that they have no known competing financial interests or personal relationships that could have appeared to influence the work reported in this paper.

Acknowledgment

We gratefully need to acknowledge the assistance of professor Alan Newman of Coventry University, for assistance in the preparation of this manuscript.

Appendix A. Supplementary data

Supplementary data to this article can be found online at https://doi.org/10.1016/j.jenvman.2021.111950.

Funding

This project has received funding from the European Union's Horizon 2020 research and innovation program under the Marie Sklodowska-Curie grant No 765057, project name SAFERUP!

References

Abdoli, M.A., Fathollahi, A., Babaei, R., 2015. The application of recycled aggregates of construction debris in asphalt concrete mix design. Int. J. Environ. Res. 9, 489–494.
Adamiec, E., Jarosz-Krzemińska, E., Wieszała, R., 2016. Heavy metals from non-exhaust vehicle emissions in urban and motorway road dusts. Environ. Monit. Assess. 188, 369.
Ali, A., Baheti, V., Militky, J., Khan, Z., Tunakova, T., Naeem, S., 2017. Copper coated multifunctional cotton fabrics. J. Ind. Textil. 48 (2), 448–464.
Alpat, Ş., Alpat, S.K., Çadirci, B.H., Özbayrak, Ö., Yasa, I., 2010. Effects of biosorption parameter: kinetics, isotherm and thermodynamics for Ni(II) biosorption from aqueous solution by Circinella sp. Electron. J. Biotechnol. 13 https://doi.org/10.2225/vol13-issue5-fulltext-20.
Amer, M.W., Ahmad, R.A., Awwad, A.M., 2015. Biosorption of Cu(II), Ni(II), Zn(II) and Pb(II) ions from aqueous solution by Sophora japonica pods powder. Int J. Ind. Chem. https://doi.org/10.1007/s40090-014-0030-8.
Andreazza, R., Pieniz, S., Wolf, L., Lee, M.K., Camargo, F.A.O., Okeke, B.C., 2010. Characterization of copper bioreduction and biosorption by a highly copper resistant bacterium isolated from copper-contaminated vineyard soil. Sci. Total Environ. 408 https://doi.org/10.1016/j.scitotenv.2009.12.017.
Arun, Jeganathan, et al., 2014. Optimization of extracellular polysaccharide production in Halobacillus trueperi AJSK using response surface methodology. African journal of biotechnology 13, 4449–4457. https://doi.org/10.5897/AJB2014.14109.
Atsdr, 2004. Public statement on copper. DEPARTMENT of HEALTH AND HUMAN SERVICES, Public Health Service Agency for Toxic Substances and Disease Registry. https://www.atsdr.cdc.gov/ToxProfiles/tp132-c1-b.pdf.
Baraka, A., 2015. Investigation of temperature effect on surface-interaction and diffusion of aqueous-solution/porous-solid adsorption systems using diffusion-binding model. J. Environ. Chem. Eng 3. https://doi.org/10.1016/j.jece.2014.11.001.
Ben-Tal, N., Honig, B., Bagdassarian, C.K., Ben-Shaul, A., 2000. Association entropy in adsorption processes. Biophys. J. 79 https://doi.org/10.1016/S0006-3495(00)76372-7.
Blanchard, G., Maunaye, M., Martin, G., 1984. Removal of heavy metals from waters by means of natural zeolites. Water Res. 18 https://doi.org/10.1016/0043-1354(84)90124-6.
Bradley, E., Winston, R., Hunt, W., Barrett, M., 2012. Water quality of drainage from permeable friction course'. J. Environ. Eng. 138, 174–181. https://doi.org/10.1061/(ASCE)EE, 1943-7870.0000476.
Brinks, M.V., Dwight, R.H., Osgood, N.D., Sharavanakumar, G., Turbow, D.J., El-Gohary, M., Caplan, J.S., Semenza, J.C., 2008. Health risk of bathing in southern California coastal waters. Arch. Environ. Occup. Health 63, 123–135.
Cerino-Córdova, F.J., García-León, A.M., Soto-Regalado, E., Sánchez-González, M.N., Lozano-Ramírez, T., García-Avalos, B.C., Loredo-Medrano, J.A., 2012. Experimental design for the optimization of copper biosorption from aqueous solution by *Aspergillus terreus*. J. Environ. Manag. 95.
Chahal, M.K., Shi, Z., Flury, M., 2016. Nutrient leaching and copper speciation in compost-amended bioretention systems. Sci. Total Environ. 556, 302–309. https://doi.org/10.1016/j.scitotenv.2016.02.125.
Chen, X.C., Wang, Y.P., Lin, Q., Ji Yan Shi, J.Y., Wu, W.X., Ying Xu Chen, Y.X., 2005. Biosorption of copper(II) and zinc(II) from aqueous solution by Pseudomonas putida CZ1. Colloids and Surfaces B: Biointerfaces. 46, 101–107.
Choińska-Pulit, A., Sobolczyk-Bednarek, J., Łaba, W., 2018. Optimization of copper, lead and cadmium biosorption onto newly isolated bacterium using a Box-Behnken design. Ecotoxicol. Environ. Saf. 149 https://doi.org/10.1016/j.ecoenv.2017.12.008.
Choudhary, Sangeeta, Sar, Pinaki, 2009. Characterization of a metal resistant Pseudomonas sp. isolated from uranium mine for its potential in heavy metal (Ni2+, Co2+, Cu2+, and Cd2+) sequestration. Bioresource Technology 100, 2482–2492. https://doi.org/10.1016/j.biortech.2008.12.015.
Costa, O.Y.A., Raaijmakers, J.M., Kuramae, E.E., 2018. Microbial extracellular polymeric substances: ecological function and impact on soil aggregation. Front. Microbiol. https://doi.org/10.3389/fmicb.2018.01636.
Coupe, S.J., Smith, H.G., Newman, A.P., Puehmeier, T., 2003. Biodegradation and microbial diversity within permeable pavements. Eur. J. Protistol. 39, 495–498.
Das, S., Dash, H.R., 2017. Handbook of metal-microbe interactions and bioremediation, handbook of metal-microbe interactions and bioremediation. https://doi.org/10.1201/9781315153353.
De Abreu C.P., Fabiano, et al., 2014. Effects of Cadmium and Copper Biosorption on *Chlorella vulgaris*. Bulletin of Environmental Contamination and Toxicology 93, 405–409. https://doi.org/10.1007/s00128-014-1363-x.
DEFRA, 2019. 'Non-Exhaust emissions from road traffic' report from the air quality expert group to the department for environment. Food and Rural Affairs; Scottish Government; Welsh Government; and Department of the Environment in Northern Ireland, on non-exhaust emissions from road traffic. https://ukair.defra.gov.uk/assets/documents/reports/cat09/1907101151_20190709_Non_Exhaust_Emissions_typeset_Final.pdf.

El-Sheikh, A.H., 2014. Partial pyrolysis of olive wood to improve its sorption of chlorophenols and nitrophenols. Int. J. Environ. Sci. Technol. 11 https://doi.org/10.1007/s13762-013-0333-x.
El-Sheikh, A.H., Abu Hilal, M.M., Sweileh, J.A., 2011. Bio-separation, speciation and determination of chromium in water using partially pyrolyzed olive pomace sorbent. Bioresour. Technol. 102 https://doi.org/10.1016/j.biortech.2011.03.021.
El-Sheikh, A.H., Fasfous, I.I., Al-Salamin, R.M., Newman, A.P., 2018. Immobilization of citric acid and magnetite on sawdust for competitive adsorption and extraction of metal ions from environmental waters. J. Environ. Chem. Eng 6, 5186–5195. https://doi.org/10.1016/j.jece.2018.08.020.
El-Sheikh, A.H., Shudayfat, A.M., Fasfous, I.I., 2019. Preparation of magnetic biosorbents based on cypress wood that was pretreated by heating or TiO2 deposition. Ind. Crop. Prod. 129 https://doi.org/10.1016/j.indcrop.2018.11.074.
Erkey, C., 2011. Supercritical fluids and organometallic compounds. From recovery of metals to synthesis of nanostructured materials.
EU, 2014. 'Non-exhaust traffic related emissions. Brake and tyre wear PM' European Commission Joint Research Centre Institute of Energy and Transpor. https://publications.jrc.ec.europa.eu/repository/bitstream/JRC89231/jrc89231-online%20final%20version%202.pdf.
Fathollahi, A., Khasteganan, N., Coupe, S.J., Newman, A.P., 2020a. A meta-analysis of metal biosorption by suspended bacteria from three phyla. Chemosphere. https://doi.org/10.1016/j.chemosphere.2020.129290.
Fathollahi, A., Coupe, S.J., El-Sheikh, A.H., Sañudo-Fontaneda, L.A., 2020b. The biosorption of mercury by permeable pavement biofilms in stormwater attenuation. Sci. Total Environ. 741 https://doi.org/10.1016/j.scitotenv.2020.140411.
Flemming, H.C., Wingender, J., 2001. Relevance of microbial extracellular polymeric substances (EPSs) - Part I: structural and ecological aspects, in: water Science and Technology. https://doi.org/10.2166/wst.2001.0326.
Freundlich, H.M.F., 1906. Over the adsorption in solution. J. Phys. Chem. 57, 385–471.
Giles, C.H., Smith, D., 1974. A general treatment and classification of the solute adsorption isotherm Part I. Theoretical. J. Colloid interface sci. 47.
Giotta, L., Mastrogiacomo, D., Italiano, F., Milano, F., Agostiano, A., Nagy, K., Valli, L., Trotta, M., 2011. Reversible binding of metal ions onto bacterial layers revealed by protonation-induced ATR-FTIR difference spectroscopy. Langmuir 27. https://doi.org/10.1021/la104868m.
Griffiths, B.S., Philippot, L., 2013. Insights into the resistance and resilience of the soil microbial community. FEMS Microbiol. Rev. https://doi.org/10.1111/j.1574-6976.2012.00343.x.
Guilhen, C., Forestier, C., Balestrino, D., 2017. Multiple elaborate strategies for dissemination of bacteria with unique properties. Mol. Microbiol. https://doi.org/10.1111/mmi.13698.
Gupta, H., Gogate, P.R., 2016. Intensified removal of copper from waste water using activated watermelon based biosorbent in the presence of ultrasound. Ultrason. Sonochem. 30 https://doi.org/10.1016/j.ultsonch.2015.11.016.
Hauser-Davis, R.A., Bastos, F.F., Tuton, B., Chávez Rocha, R., Pierre, T., Ziolli, R.L., Arruda Marco, A.Z., 2014. Bile and liver metallothionein behavior in copper-exposed fish. J. Trace Elem. Med. Biol. 28 (1), 70–74.
He, Sufang, Han, C., Wang, H., Zhu, W., He, Suyun, He, D., Luo, Y., 2015. Uptake of arsenic(V) using alumina functionalized highly ordered mesoporous SBA-15 (Alx-SBA-15) as an effective adsorbent. J. Chem. Eng. Data 60. https://doi.org/10.1021/je500978k.
Ho, Y.S., McKay, G., 1998. A Comparison of chemisorption kinetic models applied to pollutant removal on various sorbents. Process Saf. Environ. Protect. 76 https://doi.org/10.1205/095758298529696.
Huang, F., Dang, Z., Guo, C.L., Lu, G.N., Gu, R.R., Liu, H.J., Zhang, H., 2013. Biosorption of Cd(II) by live and dead cells of Bacillus cereus RC-1 isolated from cadmium-contaminated soil. Colloids Surfaces B Biointerfaces 107. https://doi.org/10.1016/j.colsurfb.2013.01.062.
Ingle, P.K., Gadipelly, C., Rathod, V.K., 2015. Sorption of copper (II) from aqueous solution onto Arachis hypogaea husk. Desalin. Water Treat 55. https://doi.org/10.1080/19443994.2014.914446.
Jin, X., Xiang, Z., Liu, Q., Chen, Y., Lu, F., 2017. Polyethyleneimine-bacterial cellulose bioadsorbent for effective removal of copper and lead ions from aqueous solution. Bioresour. Technol. 244 https://doi.org/10.1016/j.biortech.2017.08.072.
Kapoor, A., Viraraghavan, T., 1997. Heavy metal biosorption sited in Aspergillus Niger. Bioresour. Technol. 61, 221–227.
Kariuki, Z., Kiptoo, J., Onyancha, D., 2017. Biosorption studies of lead and copper using rogers mushroom biomass Lepiota hystrix. South African J. Chem. Eng. 23 https://doi.org/10.1016/j.sajce.2017.02.001.
Kyzas, G.Z., Matis, K.A., 2015. Nanoadsorbents for pollutants removal: a review. J. Mol. Liq. https://doi.org/10.1016/j.molliq.2015.01.004.
LaBarre, W.J., Ownby, David R., Lev, S.M., Rader, Kevin J., Casey, Ryan E., 2016. Attenuation of copper in runoff from copper roofing materials by two stormwater control measures. Water Res. 88, 207–215. https://doi.org/10.1016/j.watres.2015.10.009.
Lagergren, S., 1898. Zur theorie der sogenannten adsorption geloster stoffe. Kungliga Sevenska Vetenskapasakademiens. Handlingar 24, 1–39.
Langeroodi, N.S., Safaei, E., 2016. Carbonized medlar-core particles as a new biosorbent for removal of Cu2+ from aqueous solution and study of its surface morphology. Water Sci. Technol. 74 https://doi.org/10.2166/wst.2016.205.
Langmuir, I., 1916. The constitution and fundamental properties of solids and liquids. Part I. Solids. J. Am. Chem. Soc. 38 https://doi.org/10.1021/ja02268a002.
Letnik, I., Avrahami, R., Port, R., Greiner, A., Zussman, E., Rokem, J.S., Greenblatt, C., 2017. Biosorption of copper from aqueous environments by Micrococcus luteus in cell suspension and when encapsulated. Int. Biodeterior. Biodegrad. 116 https://doi.org/10.1016/j.ibiod.2016.09.029.
Liu, J., Hexiang, Y., Ziyuan Liao, Z., Zhang, K., Schmidt, R., Tao, T., 2019. Laboratory analysis on the surface runoff pollution reduction performance of permeable pavements. Sci. Total Environ. 1–8. https://doi.org/10.1016/j.scitotenv.2019.07.028.
Majumdar, P., Khan, A.Y., Bandyopadhyaya, R., 2016. Diffusion, adsorption and reaction of glucose in glucose oxidase enzyme immobilized mesoporous silica (SBA-15) particles: experiments and modeling. Biochem. Eng. J. 105 https://doi.org/10.1016/j.bej.2015.10.011.
Mckenzie, E.R., Money, J.E., Green, P.G., Young, T.M., 2009. Metals associated with stormwater-relevant brake and tire samples. Sci. Total Environ. 407 (22), 5855–5860.
Michels, H.T., Boulanger, B., Nikolaidis, N.P., 2002. Copper roof storm water runoff. Corrosion and the Environment. In CORROSION 2002. NACE International. https://www.copper.org/environment/impact/NACE02225/.
Müller, A., Österlund, H., Marsalek, J., Viklander, M., 2020. The pollution conveyed by urban runoff: a review of sources. Sci. Total Environ. 709, 136125.
Nederlof, M.M., Riemsdijk, W.H., Haan, F.A.M., 1993. Effect of ph on the bioavailability of metals in soils. https://doi.org/10.1007/978-94-011-2008-1_45, 215, 219.
NOAA, 2007. An overview of sensory effects on juvenile salmonids exposed to dissolved copper: applying a benchmark concentration. Approach to evaluate sublethal neurobehavioral toxicity. U.S. Department of Commerce National Oceanic and Atmospheric Administration. National Marine Fisheries Service, NOAA Technical Memorandum NMFS-NWFSC-83.
NOAA, 2020. Coho Salmon (protected), species directory. Fish and Wildlife Servicehttps://www.fws.gov/endangered/laws-policies/. https://www.fisheries.noaa.gov/species/coho-salmon-protected.
NRC, 2000. Health effects of excess copper' copper in drinking water. National Research Council (US) Committee on Copper in Drinking Water. Washington (DC): National Academies Press (US) 2000. https://www.ncbi.nlm.nih.gov/books/NBK225400.
O'Hayrene, R., 2014. Materials Kinetics Fundamentals. John Wiley & Sons.
Peña, J., Bargar, J.R., Sposito, G., 2011. Role of bacterial biomass in the sorption of Ni by biomass-birnessite assemblages. Environ. Sci. Technol. https://doi.org/10.1021/es201446r.
Peters, D.T., 1999. New research on runoff from copper roofs. Copper Applications in Health & Environment. https://www.copper.org/publications/newsletters/innovations/1999/04/conn.html.
Putra, W.P., Kamari, A., Yusoff, S.N.M., Ishak, C.F., Mohamed, A., Hashim, N., Isa, I.M., 2014. Biosorption of Cu (II), Pb(II) and Zn (II) ions from aqueous solutions using selected waste materials: adsorption and characterisation studies. J. Encapsulation Adsorpt. Sci. 4 (4), 201–213.
Russo, V., Tesser, R., Masiello, D., Trifuoggi, M., Di Serio, M., 2016. Further verification of adsorption dynamic intraparticle model (ADIM) for fluid-solid adsorption kinetics in batch reactors. Chem. Eng. J. 283 https://doi.org/10.1016/j.cej.2015.08.066.
Sakson, G., Brzezinska, A., Zawilski, M., 2018. Emission of heavy metals from an urban catchment into receiving water and possibility of its limitation on the example of Lodz city. Environ. Monit. Assess. 190 (5) https://doi.org/10.1007/s10661-018-6648-9.
Schipper, B.W., Lin, H.C., Meloni, M.A., Wansleeben, K., Heijungs, R., van der Voet, E., 2018. Estimating global copper demand until 2100 with regression and stock dynamics Resources Conservation and Recycling, 132, 28–36.
Shiyab, S., 2018. Phytoaccumulation of copper from irrigation waterand its effect on the internal structure of lettuce. Agriculture 8, 1–13.
Shroff, K.A., Vaidya, V.K., 2011. Kinetics and equilibrium studies on biosorption of nickel from aqueous solution bydead fungal biomass of Mucor hiemalis. Chem. Eng. J. 171, 1234–1245. https://doi.org/10.1016/j.cej.2011.05.034.
Simonin, J.P., Bouté, J., 2016. Intraparticle diffusion-adsorption model to describe liquid/solid adsorption kinetics. Rev. Mex. Ing. Quim. 15.
Singh, S., Singh, S.K., Chowdhury, I., Singh, R., 2017. Understanding the mechanism of bacterial biofilms resistance to antimicrobial agents. Open Microbiol. J. https://doi.org/10.2174/1874285801711010053.
Suazo-Madrid, A., Morales-Barrera, L., Aranda-García, E., Cristiani-Urbina, E., 2011. Nickel(II) biosorption by rhodotorula glutinis, in: journal of industrial microbiology and biotechnology. https://doi.org/10.1007/s10295-010-0828-0.
Tapiero, H., Townsend, D.M., Tew, K.D., 2003. Trace elements in human physiology and pathology. Copper. Biomed. Pharmacother. https://doi.org/10.1016/S0753-3322(03)00012-X.
Taragini, K., Satpathy, G.R., 2009. Optimization of heavy metal biosorption using attenuated cultures of Bacillus subtilis and Pseudomonas aeruginosa. Journal of environmental research and development 3, 677–684.
Tegenaw, A., Sorial, G.A., Sahle-Demessie, E., Han, C., 2019. Characterization of colloid-size copper-based pesticide and its potential ecological implications. Environ. Pollut. 253, 278–287.
Ucun, H., Aksakal, O., Yildiz, E., 2009. Copper(II) and zinc(II) biosorption on Pinus sylvestris L. J. Hazard Mater. 161 https://doi.org/10.1016/j.jhazmat.2008.04.050.
USFWS, 2020. Endangered species Act: overview. U.S. Fish and Wildlife Service. https://www.fws.gov/endangered/laws-policies/.
Vullo, D.L., Ceretti, Helena M., Daniel, M.A., Silvana, A.M., Ramirez, S.A.M., Zalts, A., 2008. Cadmium, zinc and copper biosorption mediated by *Pseudomonas veronii* 2E. Bioresour. Technol. 99, 5574–5581.
Weber, W., 1963. Kinetics of adsorption on carbon from solution. J. Sanit. Eng. Div. 89.
Whitfield, J.B., Dy, V., Mcquilty, R., Zhu, G., Heath, A.C., Montgomery, G.W., Martin, N. G., 2010. Genetic effects on toxic and essential elements in humans: arsenic, cadmium, copper, lead, mercury, selenium, and zinc in erythrocytes. Environ. Health Perspect. 118, 776–782.

World Health Organisation, 2004. *Copper in drinking-water: Background document for development of WHO Guidelines for drinking-water quality.* WHO/SDE/WSH/03.04/88. https://www.who.int/water_sanitation_health/dwq/chemicals/copper.pdf.

Wu, Y., Zeng, J., Zhu, Q., Zhang, Z., Lin, X., 2017. PH is the primary determinant of the bacterial community structure in agricultural soils impacted by polycyclic aromatic hydrocarbon pollution. Sci. Rep. 7 https://doi.org/10.1038/srep40093.

Xia, L., Xu, X., Zhu, W., Huang, Q., Chen, W., 2015. A comparative study on the biosorption of Cd2+ onto Paecilomyces lilacinus XLA and Mucoromycote sp. XLC. Int. J. Mol. Sci. 16 https://doi.org/10.3390/ijms160715670.

Xu, H., Tay, J.H., Foo, S.K., Yang, S.F., Liu, Y., 2004. Removal of dissolved copper(II) and zinc(II) by aerobic granular sludge. Water Sci. Technol. 50 https://doi.org/10.2166/wst.2004.0559.

Yang, Y., Hu, M., Zhou, D., Fan, W., Wang, X., Huo, M., 2017. Bioremoval of Cu2+ from CMP wastewater by a novel copper-resistant bacterium Cupriavidus gilardii CR3: characteristics and mechanisms. RSC Adv. 7 https://doi.org/10.1039/c7ra01163f.

Yin, W., Wang, Y., Liu, L., He, J., 2019. Biofilms: the microbial “protective clothing” in extreme environments. Int. J. Mol. Sci. 20 https://doi.org/10.3390/ijms20143423.

Zhang, D., Zhang, S., Zhang, W., Gu, J., Liu, Q., Su, H., 2018. Morphology genetic materials templated from nature species. Mater. China 37. https://doi.org/10.7502/j.issn.1674-3962.2018.10.03.